ACTA IMEKO
ISSN: 2221-870X
September 2026, Volume 15, Number 3, 1 - 13

Development of an IoT-based network for urban environmental monitoring in a vulnerable area of Los Ríos, Santo Domingo, Dominican Republic

Jesús D´Alessandro[1], Melisa Vargas[1], Alfredo Sguglio[2], Pierpaolo Filippelli[2], Angelo Maciletti[3], David Feliz[3]

[1] *Instituto de Diseño para los Trópicos and Escuela de Arquitectura de UNIBE, Universidad Iberoamericana (Unibe), Av. Francia 129, 10201 Gazcue - Santo Domingo, Dominican Republic*
[2] *Mechanical Energetic and Management Engineering Department, University of Calabria - UNICAL, P. Bucci 46/c, 87036 Calabria, Italy*
[3] *Smart City Instruments Spin Off Universita della Calabria, Mechanical Energetic and Management Engineering Department, University of Calabria - UNICAL, P. Bucci 46/c, 87036 Calabria, Italy*

ABSTRACT
The aim of this research phase was to develop an environmental data collection tool specific for the context of Los Ríos–Santo Domingo, where vulnerable settlements coexist with other clusters of higher socioeconomic status. The design of such tool needed to address the social, legal, and climatic frameworks of its context, while also aiming at a reliable, energy efficient, and replicable architecture. The project hopes to encourage future information-based participatory planning aimed at improving safety and elevating the quality of life in the area. The workflow carried out during this phase included: area visits, document consultation, work on an urban footprint map, review of comparable projects, device development, and the strategic selection of the installation site. The project achieved the design and production of ten compact devices that contain seven sensors each, to register concentrations of important air contaminants, vibration, sound intensity, and specific atmospheric conditions. Devices were installed within the inner perimeter of a property in the proximity of vulnerable and non-vulnerable polygons to enable the observation of potential reading differences. Preliminary total averages obtained from a sample showed high concentrations of CO, NO_2 (according to guidelines from WHO), and PM_1 (following the 2024 paper "On the safe levels of micro-sized particles PM1.0 in ambient air" by Zaitseva, Kleyn, Chetverkina, Andrishunas, and Tsinker), alongside noise levels between 6.9 and 74.09 dB in most units and RH values below 40 %.

Section: RESEARCH PAPER

Keywords: urban sensors; smart cities; sustainable development; information technologies; measurement; environmental research; air pollution; IoT

Citation: J. D´Alessandro, M. Vargas, A. Sguglio, P. Filippelli, A. Maciletti, D. Feliz, Development of an IoT-based network for urban environmental monitoring in a vulnerable area of Los Ríos, Santo Domingo, Dominican Republic , Acta IMEKO, vol. 15 (2026) no. 3, pp. 1-13. DOI: 10.21014/actaimeko.v15i3.2058

Section Editor: Francesco Lamonaca, University of Calabria, Italy

Received January 24, 2025; **In final form** August 20, 2026; **Published** September 2026

Funding: This Project is funded by the FONDO NACIONAL DE INNOVACIÓN Y DESARROLLO CIENTÍFICO Y TECNOLÓGICO (FONDOCYT), República Dominicana, Subvención No. 2022-3A2-154/ Mandatory note in Spanish by contract: *"Proyecto financiado por el FONDO NACIONAL DE INNOVACIÓN Y DESARROLLO CIENTÍFICO Y TECNOLÓGICO (FONDOCYT), República Dominicana, Subvención No. 2022-3A2-154"*

Corresponding author: Jesús D´Alessandro, e-mail: j.dalessandro@unibe.edu.do

1. INTRODUCTION

This article summarizes the first phase of the project "Modelo de Información Urbana (CIM) en Distrito Nacional para Mejorar su Resiliencia, Prevenir Desastres y Administrar su Espacio", code number 2022-3A2-154, which is funded by the Dominican Republic´s Fondo Nacional de Innovación y Desarrollo Científico y Tecnológico (FONDOCyT).

1.1. Urban context

The Dominican Republic and its capital city, Santo Domingo de Guzmán, are respectively among the fastest growing national and urban economies of The Americas 1), 2). In Santo Domingo de Guzmán (Distrito Nacional), this economic dynamism comes with important challenges. A historic deficit in affordable housing has taken place, while informal vulnerable settlements have expanded in the territory 3). These vulnerable settlements

Figure 1. Images of a nearby vulnerable settlement and its stream in Los Ríos.

concentrate poverty 4), often in high population densities 6.2, and comprise around a 9 % of the city´s footprint 1). In parallel, the city is heavily reliant on and overcrowded by motorized vehicles (more than one per resident, regardless of age or condition) 2).

Los Ríos is a territorial unit in Santo Domingo de Guzmán, which by 2010 had a population density of 15,062 inhabitants per square kilometre 6.2 (higher than the city average at the time of about 10,544.8 inhabitants per square kilometre 6.2). The area contains a significant vulnerable settlement footprint 3), and many of these settlements are located along natural streams of water that characterize the ecosystems of the National District´s northwest area called Circunscripción 2. Currently, the water streams are polluted, posing a significant risk for these populations. In Gran Santo Domingo, historically, rivers, aquifers, and the waterfront have been used as final receptors of polluted waters, causing systemic contamination 6.3, Figure 1.

1.2. Importance of data collection systems

Often, vulnerability is assessed only by poverty standards, focused mainly on income and physical aspects that include housing conditions. However, the quality of urban soil, waters, and air, as well as intangible factors like noise or temperature need to be assessed in order to map vulnerability comprehensively.

In the Dominican Republic, short-lived climate pollutants like carbon monoxide (CO), nitrogen oxides, and particulate matters 2.5 and 10 (PM2.5 and PM10), are expected to increase notably by 2030 1). In addition, it is important to consider that other gaseous pollutants like ammonia (NH3) and volatile organic compounds (VOC) can be expected to increase, too, since they also add to PM2.5 and PM10 concentrations 1). Air pollution is known to be able to harm the health, and consequently, the economy of individuals and families at a social scale, besides costing taxpayers money in public health services 2), 3). In contrast, there is still a need for significant data collection infrastructure to systematically register information about the urban environment in Dominican cities.

Thus, this project contributes to a culture of data collection, as it involved designing and installing devices to obtain a body of environmental information in a specific urban area, being able to expand sustainable development literature and inform planning initiatives. Additionally, the project helps gain valuable knowledge on how to develop devices and networks to monitor air pollution in urban areas in the Dominican Republic. Furthermore, without being a qualitative or social research, this project helps pave the way to future local research aiming at integrating similar methodologies to social approaches and social sciences 6.4, 7.

The significance of integrating advanced technological tools with a social and interdisciplinary approach has been previously underscored by Sguglio et al. 7.1. Their work in the RES NOVAE project demonstrates how the combination of engineering research and social sciences can enhance urban resilience. Such an approach enables the design of data collection systems to also support future participatory planning, ensuring that technological advancements deliver tangible benefits to vulnerable communities 7.1.

1.3. Previous projects

In the last decade, comparable endeavours have been carried out in different latitudes and scales yielding beneficial results. Among them are The Array of Things in Chicago, the US spanning SAGE project, and the Breath London network in London. In the context of the Dominican Republic, previous projects include “Contaminación atmosférica en puntos seleccionados de la ciudad de Santo Domingo, República Dominicana” and “Monitoreo y caracterización de los contaminantes atmosféricos a través de una red inalámbrica de sensores en las ciudades de Santo Domingo y Santiago de los Caballeros en la República Dominicana”.

The Array of Things (AoT) started in 2016 and managed to generate a publicly available dataset spanning four years of data collection in Chicago, IL, USA. The project comprised sensor hubs inside compact cases installed around the city. Each unit contained over 12 sensors. Initially, 500 units were planned to be installed in Chicago by 2018. The set of units was configured as a network connected to the Internet and was based on an open platform called Waggle, which manages edge-computing wireless sensors that are “intelligent” 7.2. The data collected included light intensity, information on air composition like concentrations of carbon dioxide (CO_2) and PM2.5, as well as meteorological measures related to heat, humidity, and temperature 7.3–7.4. In addition to the usefulness of the body of information collected, helping the city to operate more efficiently, the project was purposed to “provide real-time, location-based data about urban environment, infrastructure and activity to researchers and the public” 7.3. Later, AoT collaborated on project Eclipse which installed 115 sensors in Chicago spots, extracting data “for over 90 % of expected sensor-hours from July 2 - September 30, 2021” 1).

In 2019, once AoT was launched, the SAGE project initiated, led by the Northwestern University in a nationwide enterprise. It developed further improved devices based on the Waggle platform with the collaboration of the AoT team. This project makes use of advance machine learning algorithms under “edge” computing. In this technology, computing takes place directly connected to sensors facilitating early detection and response. One important feature of this technology is the monitoring of cloud motion and aerosols, facilitating action against potential disasters like wildfires. The technology can also facilitate the observation of wildlife with research purposes, as well as the detection of radiological and nuclear activity. SAGE operated and integrated 120 devices which are AI-enabled 2)–9.

The Breathe London network is an urban air monitoring initiative for London, launched in 2019, which is managed by the Imperial College London´s Environmental Research Group. This institution researches the impact of air pollution on health. From 2020, in a new phase planned to last four more years, funding was provided to install 100+ sensors in public interest spots, from hospitals to schools to co-location sites, along the geography of the city. Looking forward to including disadvantaged demographic groups, Bloomberg Philanthropies donated funds to the project 10, [1].

The 2014 project "Contaminación atmosférica en puntos seleccionados de la ciudad de Santo Domingo, República Dominicana" consisted of the measurement and comparative analysis of air components in three major avenue intersections of Santo Domingo during May 2013. The study focused on monitoring sulphur dioxide (SO_2), nitrogen dioxide (NO_2), CO, as well as PM2.5 and PM10. Concentrations of SO_2 and NO_2 were found above the permitted limits as established by the norms of the Ministry of the Environment and Natural Resources of the Dominican Republic [2].

In 2020, the project "Monitoreo y caracterización de los contaminantes atmosféricos a través de una red inalámbrica de sensores en las ciudades de Santo Domingo y Santiago de los Caballeros en la República Dominicana" installed a network of sensors in the two major Dominican cities: Santo Domingo and Santiago. The project monitored CO, SO_2, ozone (O_3), PM2.5, and PM10, and in 2023 published preliminary results. The project states that between 2015 and 2019, in the Dominican Republic, average values of PM2.5 and PM10 were above the harmful levels established by the World Health Organization (WHO). Preliminary measurements in three different locations inside Santo Domingo, between November 2021 and February 2022 "confirm this tendency for particulate matter" [3].

These projects provide or have provided an effective social service as they monitor and register environmental conditions for the safety of populations. In parallel, their respective bodies of information can help the scientific community and governments to better comprehend, and plan for, sustainable development. Another common element among most of these projects is a network configuration operating under IoT platforms.

The following sections discuss the work carried out in our project in order to achieve the conclusion of its first phase. Section 2 will describe the site-related work, including considerations about site selection, device proximity, and wind direction. Sections 3 and 4 will present the process and characteristics of device design focusing on hardware and system architecture. Sections 5 to 7 discuss metrological matters of the sensors and the system: measurement, validation, and performance evaluation, respectively. Further on, Section 8 summarises preliminary results, followed by a note on data analysis in Section 9 and conclusions in Section 10.

2. SITE WORK

Our team visited and studied the complex urban cluster of Los Ríos (*The Rivers*) [original in Spanish]. We observed that the urban area contains densely populated vulnerable sites, a number of them built precariously over natural water streams (hence the name). These streams now run contaminated waters, since they are used as sewerage. In contrast, Los Ríos also hosts upper middle- and high-class residential areas, as well as commercial and institutional facilities.

2.1. Location for installation

Initially, our team considered installing the devices directly in a vulnerable settlement, for which it visited the place and met community members, achieving a better understanding of the context that helped inform the work. Later on, concerns about safety, maintenance, and stable energy supply of the devices arose.

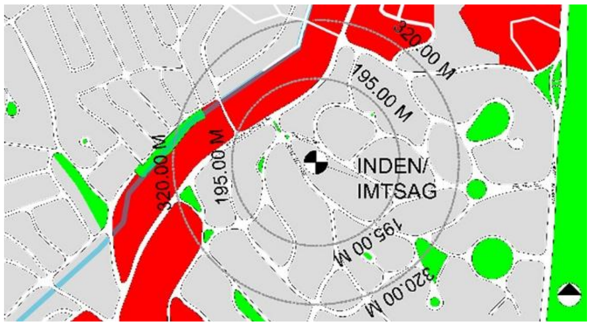

Figure 2. Site location on urban footprint map, general street fabric shown. Red footprint indicates mostly vulnerable settlements, grey is mostly non-vulnerable, and green represents mostly vegetation areas. The blue line indicates the approximate course of Arroyo Hondo water stream on Figure 1. Illustrative map drawn over maps of Google Maps.

While looking for a more convenient location, we found it important to monitor the environmental conditions of the area from a location that could relate geographically to both vulnerable and non-vulnerable settlements. This characteristic would facilitate the exploration of possible differences in the readings between areas.

Thus, we selected a land plot at coordinate 18.49239, -69.96491, where the National Institute of Diabetes, Endocrinology and Nutrition (INDEN) [for its capitals in Spanish] is located together with the Global Health and Tropical Medicine Institute (IMTSAG) [for its capitals in Spanish], see Figure 2. Conveniently, the complex is related to the Universidad Iberoamericana and is geographically near the centre of Los Ríos polygon. The property´s centre is approximately 230 metres from the Arroyo Hondo water stream (see water stream in Figure 2 and Figure 3), and around 607 m from the Botanical Garden´s property.

As can be seen in the urban footprint map in Figure 2, already within a radius of 320 m, the chosen installation site has vulnerable areas to its west and north flanks (coloured in red), and formal upper middle- and high-class housing areas on its east side (coloured in grey). Once the project had obtained the permission by INDEN, and the development–production of the devices had been finished, they were brought and installed inside the property, surrounding the buildings, outside them (see Figure 3). Eight devices were fixed in the property´s lampposts, and two on facade walls. Lampposts proved to be the most convenient elements on which to locate the devices, since they are already fed by power lines. Devices 6, 7, 8, 9, and 5 were installed facing Paseo del Yaque street, while devices 3, 4, 1, and 2 were installed facing Majoma street, and device 10 was located

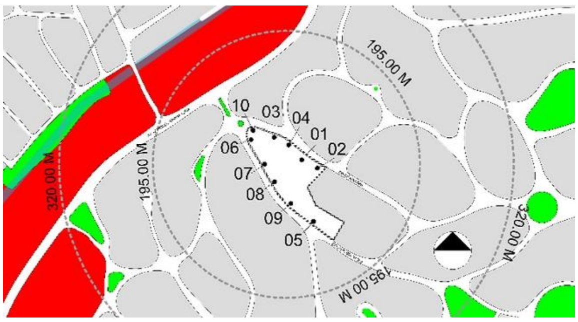

Figure 3. Numbered data collection units installed inside the INDEN/IMTSAG property, on urban footprint map (see Figure 2 for footprint description). Arroyo Hondo water stream course marked by blue lines. Illustrative map drawn over maps of Google Maps.

in the northwest corner of the property (see Figure 3). All devices were installed above human reach to prevent vandalism. All devices were additionally protected from heavy rain by loose and ventilated, hard plastic visor-coats.

The surface of interest for this study was about 1.5 square kilometres, while publicly available databases, like NASA POWER, have a resolution of 0.5 by 0.625 degrees for meteorology parameters (55.5 x 68.75 km) [4], [5]. Seemingly, the Global Forecast System (GFS27) has a resolution of 0.25 degrees (27 km) [5], and shows shifting winds in the area, tending to come from the northeast and northwest quadrants. In combination with this major resolution limitation, the uneven topography in the area, as well as numerous buildings and trees add to a complex wind circulation pattern.

2.2. Device proximity

A notable feature of this project is the high density of data collection devices. Devices were installed and aligned outside and around the buildings of the property, facing the streets (see Figure 3), separated by an approximate average distance of 33.70 meters among devices in a line. This configuration allows to explore possible environmental changes with more definition.

3. DEVICE HARDWARE

The research and prototyping of the device took place initiating with a two-board unit where sensors and other components were connected inside a temporary conventional grey box (see Figure 4). Local legislation limits and regulates the use of cameras; therefore, no cameras were incorporated in this project.

After a process of site visits, improvement, testing, and consultation with technical experts from the University of Calabria and the communications company Altice Dominicana, an improved prototype was achieved with a simpler one-board architecture. The board is connected to the data collection sensors and other components that include a surge protector to address local service instability and electric storms, and a SIM card slot to work on an IoT basis (see Figure 5 and Figure 6). The case was redesigned to improve structural resistance and to allow air intake through horizontal openings. Draining holes in the bottom can expel storm water if it filters in. To be adaptable, the flat back includes top and bottom flaps with screw holes. This facilitates fixing to either lampposts or walls (see Figure 7 to Figure 9).

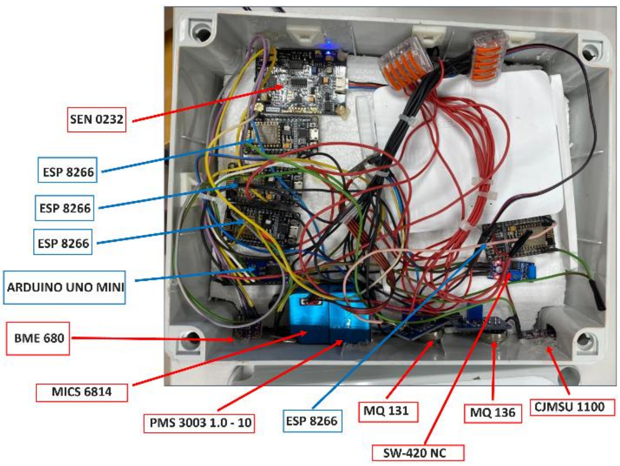

Figure 4. First prototype of the unit.

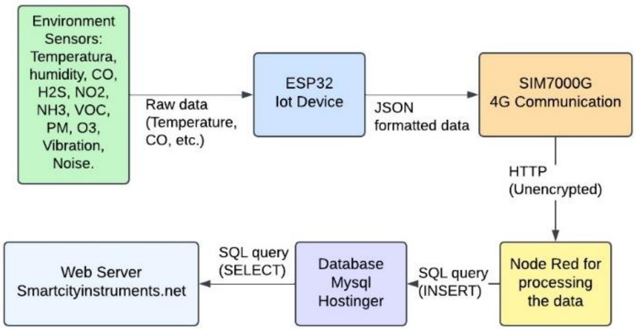

Figure 5. Evolving architecture of the system.

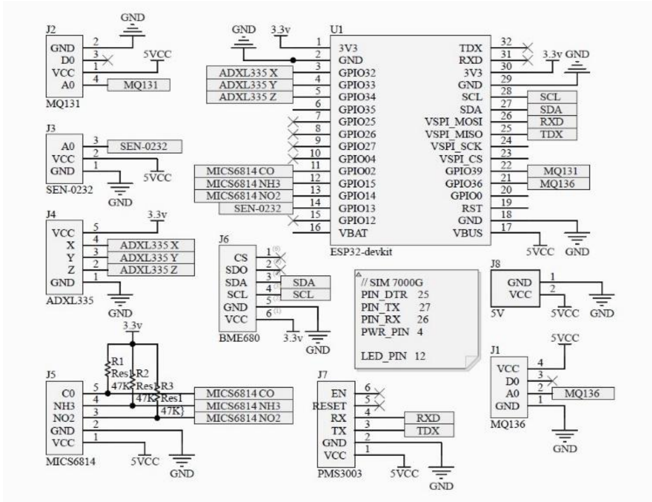

Figure 6. Connection of the prototype.

3.1. Sensors

Each compact data collection device integrates seven sensors, selected to monitor both atmospheric pollutants and environmental parameters estimated relevant to the urban context of Los Ríos–Santo Domingo. The sensor selection criteria included: relatively low power consumption for

Figure 7. Case design for the second prototype.

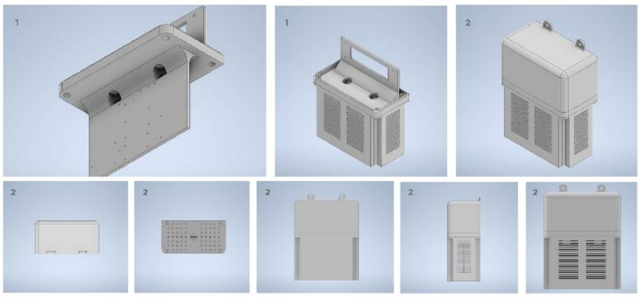

Figure 8. Views of case design for the second prototype.

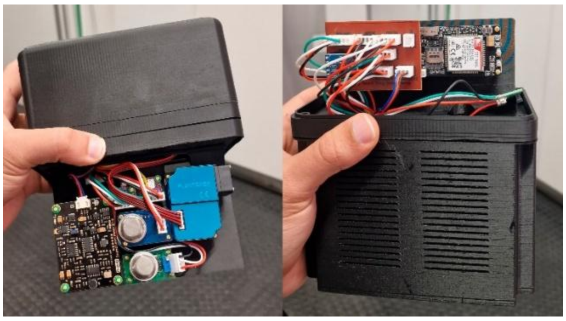

Figure 9. Electronic parts of the second prototype.

continuous operation and availability of modules suitable for IoT deployment. The combination of these sensors provides a multi-parameter characterization of the local environment.

The sensors inside the devices are: MQ136 [6], MQ131 [7], SEN0232 [8], ADXL335 [9], MICS6814 (or CJMCU6814) [10], BME680 [11], and PMS3003 [12], see Figure 6. These components register the presence of hydrogen sulphide (H_2S) or "sewer gas" [13], [14], ozone (O_3)—one of the main air pollutants causing smog—[15], ammonia (NH_3) [16], which can be expected in hazardous waste sites and contributes to particle formation [17], nitrogen dioxide (NO_2), carbon monoxide (CO), volatile organic compounds (VOCs), and particulate matter (PM)—formed anthropogenically from emissions of combustion engines in vehicles, power generators, and the broad fossil fuel industry—[18]–[21], vibration, sound intensity, temperature, and humidity. See Table 1 and Table 2.

4. ARCHITECTURE

The system architecture was designed to guarantee reliable data acquisition, energy efficiency, and secure transmission in the context of Los Ríos–Santo Domingo. It comprises four main layers: sensing hardware, communication, server processing, and visualization.

4.1. Sensing hardware layer

Inside each compact unit, the sensors are connected to a custom PCB that includes:

1) a microcontroller (ESP32-based) for data acquisition and local processing;
2) a SIM card module for IoT cellular communication;
3) power management circuits, including surge protection against local service instability and electrical storms;
4) a waterproof case with horizontal intake slots for air circulation and drainage holes for heavy rain.

4.2. Communication layer

Data collected from each unit are transmitted in near real-time via cellular IoT (through SIM cards provided by Altice Dominicana). The communication protocol is based on lightweight TCP/IP requests compatible with IoT devices.

4.3. Server processing layer

An intermediate server was configured to receive all incoming data. The server runs the visual programming tool Node-RED, which allows modular programming of data flows, preprocessing, and flexible modification when necessary. This layer also handles timestamping, initial filtering, and the aggregation of 10-minute samples into 30-minute averages.

4.4. Visualization and storage layer

Processed data are forwarded to the online platform smartcityinstruments.net. This platform provides:

1) real-time dashboards with the latest values;
2) historical data visualization with graphs and export options;
3) secure access through user accounts to guarantee data integrity.

The information flow follows the order: sensors, microcontroller/PCB, IoT SIM transmission, Node-RED

Table 1. Technical details and metrological characteristics of the sensors used.

Sensor	Target variables	Measurement range	Resolution/ Sensitivity	Notes on performance
MQ136	Hydrogen sulfide (H_2S)	1–200 ppm	< 1 ppm	Semiconductor gas sensor, responsive to "sewer gas"; baseline drift with humidity and temperature, requires periodic calibration.
MQ131	Ozone (O_3)	10 ppb–2 ppm	< 10 ppb	Semiconductor sensor with high sensitivity to O_3; response time < 90 s; affected by humidity variations.
SEN0232 (DFRobot)	Sound level (Noise in dB)	30–130 dBA	± 1.5 dB	A-weighted measurement; frequency response 31.5 Hz–8.5 kHz; response time 125 ms; adequate for relative noise monitoring in urban contexts, though not a certified Class 1/2 instrument.
MiCS6814 (CJMCU-6814)	CO, NH_3, NO_2	CO: 1–1000 ppm; NH_3: 1–500 ppm; NO_2: 0.05–10 ppm	CO sensitivity ~1 ppm; NH_3 ~1 ppm; NO_2 ~0.05 ppm	Multi-channel electrochemical gas sensor; requires compensation for T/H; cross-sensitivity possible between gases.
PMS3003	PM1, PM2.5, PM10	0–1000 µg/m³ (≥1000 max)	1 µg/m³	Accuracy ± 10 % (100–500 µg/m³) or ± 10 µg/m³ (0–100 µg/m³); laser scattering sensor; single response < 1 s, total response < 10 s; factory calibrated.
BME680 (Bosch)	Temperature, Humidity, VOC index	-40–85 °C; 0–100% RH; IAQ 0–500	Temp ± 0.5 °C; RH ± 3 %	Combines T/H with VOC measurement via MOS sensor; suitable for IAQ estimation.
ADXL335	Vibration (X, Y, Z axes)	± 3 g	300 mV/g	Analog MEMS accelerometer; used to detect vibration from traffic or structural disturbances.

Table 2. Measurement parameters and units.

Parameter	Sensor	Unit	Sampling frequency	Averaging interval	Notes
H_2S	MQ136	ppm	1 sample / 10 min	30 min	Baseline drift compensated through averaging.
O_3	MQ131	ppm	1 sample / 10 min	30 min	Sensitive to humidity; values stabilized by averaging.
CO, NO_2, NH_3	MiCS6814	ppm	1 sample / 10 min	30 min	Multi-channel electrochemical sensing; averaging reduces cross-sensitivity artifacts.
PM1, PM2.5, PM10	PMS3003	µg/m³	1 sample / 10 min	30 min	Laser scattering sensor; averaging smooths traffic-related short-term peaks.
Temp., RH, VOC index	BME680	°C, %RH, IAQ index	1 sample / 10 min	30 min	Provides contextual atmospheric baseline.
Noise level	SEN0232	dBA	Continuous, averaged to 10 min	30 min	A-weighted; ± 1.5 dB error; final data reported as 30-min mean.
Vibration	ADXL335	Trigger event	Event-based	N/A	Configured only for earthquake detection. No seismic activity was recorded during the measurement campaign.

server, and online visualization platform. This architecture balances scalability (units can be added without altering the system), reliability (redundant nodes enable comparative analysis), and adaptability (software updates on the server allow protocol modifications without physical intervention on devices).

5. MEASUREMENTS

The environmental data collection units were configured to operate under a standardized sampling cycle across the ten deployed devices. Each sensor performed a measurement every 10 minutes, and the resulting values were subsequently averaged over 30-minute intervals. This strategy reduced data noise, balanced sensor drift, and optimized energy consumption while maintaining adequate temporal resolution for urban environmental monitoring.

In collaboration with the Universidad Iberoamericana for the matter, the devices were developed and built by Smart City Instruments–University of Calabria (Calabria, Italy). Their data transmission capabilities were tested in order to ensure that the collected information would be broadcasted effectively over the Internet (see Figure 10).

5.1. Web platform

In summary, the platform was designed to work in two levels. The first one is an intermediate server that receives the data stamped and transmitted from the devices via IoT SIM cards.

The server is configured to implement the programming tool Node-RED. Then, the data is sent to the second level of the platform (smartcityinstruments.net), where all the data collected from the installed devices can be visualized. It stores both raw 10-minute values and processed 30-minute averages. This second level allows for the generation of reports containing historical data from selected devices, the visualization of the latest readings, and the display of graphics (see Figure 10). It is also equipped with a user access system to ensure data security.

This configuration ensured a compromise between temporal resolution and data reliability, allowing the detection of diurnal patterns (e.g., traffic-related peaks in PM and noise) while avoiding redundant fluctuations and sensor noise. The vibration channel remained inactive throughout the campaign, as no seismic events occurred.

6. VALIDATION

Validation procedures were implemented to ensure the reliability of the measurement chain, covering the complete process from sensor data acquisition to online visualization. The validation strategy focused on three levels: functional validation, transmission validation, and consistency checks.

6.1. Functional validation of sensors

The functional sensor validation involved the following actions:

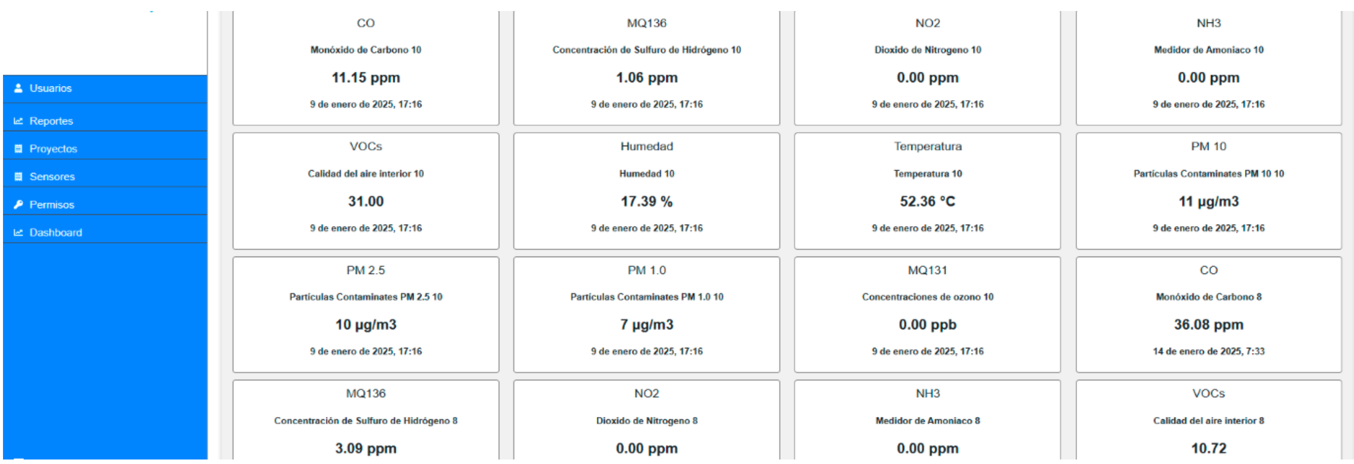

Figure 10. Data transmission test.

1) each unit was tested individually to verify that all sensors responded within their specified ranges when exposed to environmental stimuli;
2) for the gas sensors (MQ136, MQ131, MiCS6814), exposure tests were conducted using controlled environments with known pollutant sources (e.g., cleaning agents or exhaust proximity) to confirm sensitivity and response;
3) the SEN0232 sound sensor was compared against a commercial handheld sound level meter in an indoor environment, yielding deviations within the manufacturer's ± 1.5 dB specification;
4) the PMS3003 particle sensor was validated by comparing readings against a reference air quality monitor during a pilot run.

6.2. Transmission validation

The validation of transmission involved the following actions:

1) a series of continuous transmission tests were performed to confirm that data packets from all ten units reached the intermediate Node-RED server;
2) Figure 10 and Figure 11 in the article illustrate one of the data transmission tests, showing the successful forwarding of real-time measurements;
3) SIM card connectivity and network stability were tested in different time windows (day/night).

6.3. Consistency checks across devices

Checks for consistency across devices involved the following actions:

1) data from multiple nodes installed in close proximity were compared to detect anomalies and outliers;
2) redundant sensing (e.g., two units recording PM2.5 under the same conditions) confirmed that variability remained within expected tolerance levels;
3) outlier detection and filtering procedures were applied at the server level to discard spurious values, particularly in low-cost gas sensors subject to drift.

Through these procedures, the measurement chain was validated end-to-end, confirming that the deployed system was capable of: capturing environmental variables within expected ranges, transmitting data reliably via cellular IoT, and storing and visualizing results without significant data loss.

6.4. Limitations of low-cost sensors and data processing

While low-cost environmental sensors—such as the MQ-series and MiCS6814 used in this project—provide a cost-effective solution for high-density spatial monitoring, they possess inherent metrological limitations. These strictly factory-calibrated components are susceptible to baseline drift, cross-sensitivity to non-target gases, and environmental dependencies.

To mitigate these limitations in the absence of quantitative in-field calibration, a two-tier data processing strategy was implemented. First, at the edge-computing level, the microcontroller firmware executes a local oversampling routine (averaging 10 consecutive samples with a 10-millisecond interval) for the analog sensors to filter out high-frequency electrical noise prior to transmission. Additionally, digital sensors like the BME680 are configured to utilize built-in oversampling and Infinite Impulse Response (IIR) filters to stabilize readings. Second, at the server level (Node-RED), the transmitted data are aggregated into 30-minute averages. This temporal aggregation significantly smooths short-term signal noise and transient anomalies. Although this dual filtering approach does not replace formal metrological calibration against reference instruments, it effectively reduces uncertainty, ensuring that the collected dataset reliably reflects relative environmental trends, peaks, and spatial differences.

Specifically, the conversion of raw analog signals to engineering units was performed at the server level using the sensitivity curves provided by the manufacturers. For the electrochemical and MOS sensors, the resistance ratio R_s/R_0 was calculated and mapped to gas concentration using a power-law regression model: $X = a(R_s/R_0)^b$, where X is the concentration and a, b are coefficients derived from each sensor's characteristic curve. This processing allows for future software-based recalibration without requiring physical access to the deployed hardware.

7. PERFORMANCE EVALUATION

The performance of the data collection system was evaluated through field deployment of the ten compact units in Los Ríos–Santo Domingo. The evaluation considered operational stability, data transmission, energy consumption, and preliminary environmental readings.

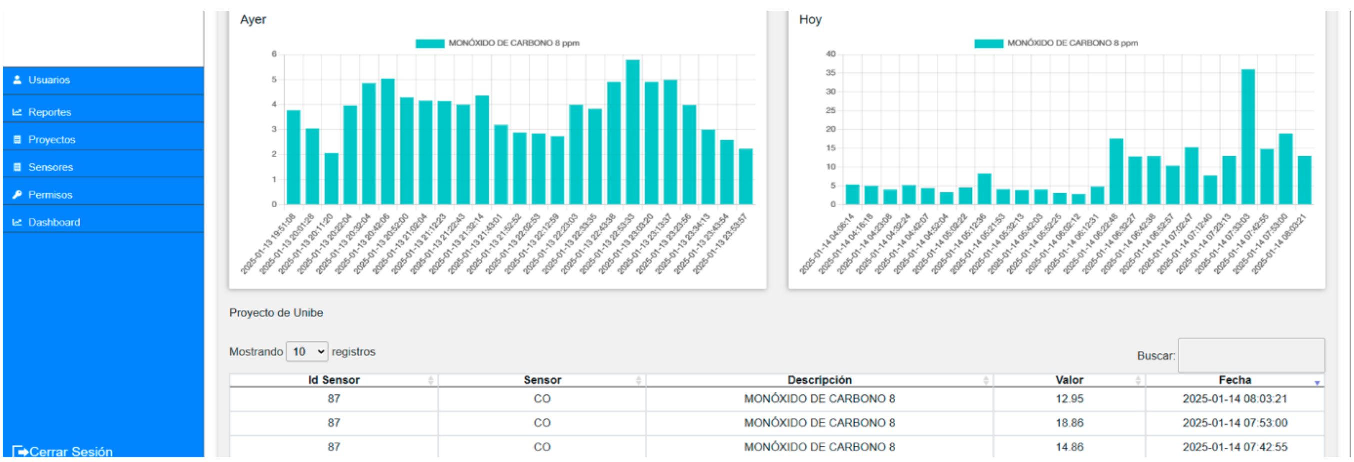

Figure 11. Data transmission test.

7.1. Operational stability

Regarding operational stability, eight out of the ten deployed units operated continuously without major failures throughout the measurement campaign. However, devices 9 and 10 experienced a permanent loss of communication a few days after their initial installation. Although physical reboots of the devices were attempted on site, they failed to re-establish the cellular IoT connection. Because the specialized technical team from Smart City Instruments had already departed the country, a deeper hardware diagnostic was unfeasible. Consequently, the exact physical root cause—whether a localized power supply issue at the lamppost, a cellular module/SIM failure, or an internal hardware fault—remains undetermined.

However, from a reliability engineering perspective, the failure of 20 % of the nodes highlights the challenges of long-term IoT deployment in tropical climates with high humidity ($RH > 90\ \%$) and electrical instability. Despite this, the spatial redundancy of the remaining 8 units ensured the integrity of the total dataset.

Device proximity (see section 2.2) provided significant spatial redundancy. The remaining eight active nodes successfully covered the target area without generating spatial blind spots, ensuring continuous and representative data collection for the analysis.

Furthermore, protective features such as the surge protector, waterproof casing, and drainage holes proved effective in all units, which functioned stably under tropical weather conditions, including heavy rainfall.

7.2. Data transmission

All units transmitted data reliably to the Node-RED server and the visualization platform. Although devices 9 and 10 later failed.

7.3. Energy performance

The following observations address the energy performance of devices:

1) average power consumption per unit was approximately 3.5 W (≈ 700 mA @ 5 V), including all sensors and the communication module;
2) the relatively high demand is primarily due to the heating elements of the MQ-series semiconductor gas sensors;
3) this consumption is fully compatible with continuous deployment using lampposts and building electrical supplies.

Energy characterization showed that the MQ heating elements represented 85 % of the total 3.5 W power demand. This confirms that while the system is IoT-capable, it requires a stable power grid connection (such as the lampposts used) rather than small-scale solar harvesting for this specific high-consumption sensor array.

7.4. Preliminary environmental performance

The following observations address preliminary environmental performance:

1) noise measurements typically ranged between moderate levels during daytime and higher levels during traffic-intensive hours, consistent with the urban soundscape of Los Ríos;
2) particulate matter (PM2.5 and PM10) showed higher values during peak traffic periods, suggesting the expected influence of vehicular emissions;
3) gas sensors (CO, NO_2, NH_3, O_3, H_2S) reported values within detectable ranges, though further calibration and validation against reference instruments are needed;
4) no seismic events were detected by the vibration sensor (ADXL335) during the deployment.

Figure 10 and Figure 11 illustrate the functionality of the data acquisition and visualization platform rather than presenting scientifically interpretable environmental results. Figure 10 shows a real-time dashboard displaying instantaneous values acquired from multiple sensors, including CO, H_2S, O_3, NO_2, NH_3, VOCs, particulate matter (PM1.0, PM2.5, PM10), temperature, and humidity. Each element includes the measured value, unit, and timestamp, confirming the correct operation of the end-to-end transmission chain (sensor → microcontroller → IoT communication → server → visualization platform). Figure 11 presents the historical data interface for a selected variable (CO in this case), including time-series visualization and tabulated records. These figures are intended to demonstrate system functionality, data integrity, timestamp synchronization, and storage capability, rather than to support quantitative environmental analysis.

The platform allows the same visualization for any of the deployed sensors. The bar charts show daily variation (yesterday vs. today), while the table at the bottom lists sensor ID, variable description, measured values, and timestamps.

This functionality confirms the platform's ability to handle both real-time monitoring and archival storage of environmental data, ensuring traceability and facilitating future analysis. See Table 3.

8. PRELIMINARY RESULTS

During the initial deployment, the ten devices successfully operated in field conditions and generated environmental datasets according to the defined measurement cycle (sampling every 10 minutes, averaged every 30 minutes). All sensors transmitted data through the IoT chain (device → Node-RED server → visualization platform), confirming end-to-end system functionality. Preliminary datasets include:

1) gas measurements (CO, NO_2, NH_3, O_3, H_2S) – values were successfully recorded within the detection ranges of the corresponding sensors (MQ131, MQ136, MiCS6814);
2) particulate matter (PM1.0, PM2.5, PM10) – continuous readings were obtained from the PMS3003 sensor, with values expressed in $\mu g/m^3$;
3) noise levels – SEN0232 provided decibel readings in the expected range (30–130 dBA), processed into 30-minute averages;

Table 3. Performance summary of the deployed system.

Metric	Result	Notes
Uptime (devices)	8 stable / 2 failed	
Data transmission	Stable in 8 devices	
Power consumption per unit	~3.5 W (≈ 700 mA @ 5 V)	Includes all sensors and communication modules.
Noise levels (SEN0232)	Variable, higher in traffic hours	Consistent with urban environment.
Particulate matter (PMS3003)	Variable, higher in peak hours	Traffic-related influence observed.
Vibration (ADXL335)	None detected	No seismic events occurred.

4) temperature and humidity – BME680 recorded atmospheric context variables, ensuring support for environmental correlation;
5) vibration – ADXL335 was active but did not register seismic events during the campaign period.

The dataset collected demonstrated that the monitoring network was fully functional and capable of producing structured, time-stamped data across all variables. These preliminary measurements served as an initial trial, being the basis for further calibration, validation, and detailed analysis in subsequent project phases.

For initial trial testing, a data sample spanning from the 10th of January 2025, to the 11th of February 2025, from all eight working devices was obtained, and factor averages were calculated for each device. See Table 4 with thresholds [13], [16], [22]–[27].

These results should be interpreted as preliminary indicators rather than absolute calibrated concentrations, since the deployed sensors were not subjected to laboratory calibration against reference instruments.

9. DATA ANALYSIS

After the phase reported in this article, a second phase took place where a final data sample was identified and analysed considering day averages for each device, focusing not only on pollutant concentration but also on possible patterns that could be linked to socioeconomic differences in the area. The data analysis in the second phase consisted of statistical analysis, representation using tables, and maps from a geographic information system platform.

10. CONCLUSIONS

During this preliminary testing period, averages for carbon monoxide (CO) ranged from 4.67 to 6.77 mg/m³, and nitrogen dioxide (NO_2) ranged from 24.97 to 25.59 μg/m³. These values exceed established WHO safety thresholds (4 mg/m³ and 10 μg/m³, respectively) [22]. Particulate matter (PM_1) values were also observed to be elevated as being above the mark of 2 μg/m³ [23], while all noise averages were above 45 dBs with only one average below 53 dBs. The averages do not show specific values for night or daytime, however, as reference, the WHO recommends a maximum limit for noise caused by road traffic of 53 dB, and of 45 dB during the night [24]. Additionally, relative humidity (RH) values were consistently logged below the 40 % optimal threshold [26].

This phase of the project successfully demonstrated the viability and critical need for a high-density IoT environmental monitoring network to better understand vulnerability in urban areas. To reflect upon the possible impact of the preliminary environmental data registered, one important aspect to consider is that devices were installed above human reach to prevent vandalism. If a major share of the gas and noise pollution in the area was originated in combustion vehicles, then gas concentrations and decibel levels could be greater at the height of engines and exhausts. However, gas and air temperatures, and wind patterns could have an impact on concentrations, too.

As for effects on human health, according to the WHO, exposure to high concentrations of carbon monoxide (CO) is associated with myocardial infarction [19], while nitrogen dioxide (NO_2) is known to be a precursor of other pollutants, and exposure to high concentrations is related to non-accidental and respiratory mortality [19]. Additionally, high levels of micro-particles, like PM1, can cause cardiovascular, respiratory diseases, as well as diseases of the immune and endocrine systems [22]. As for high noise levels, according to the WHO, exposure can have "cardiovascular and metabolic effects; annoyance; effects on sleep; cognitive impairment; hearing impairment and tinnitus; adverse birth outcomes; and quality of life, mental health and wellbeing." [24] (p. xiv).

Thus, vulnerability by environmental pollution needs to be understood as a challenge that might affect populations of different socioeconomic status (SES). However, it is important to explore a possible relationship between SES and environmental pollution. Hence, the second phase of this project focuses not only on pollutant concentration but also on possible patterns that could be linked to socioeconomic differences in the area.

For this particular sample, Table 5 and Figure 12 show higher average values per certain variables among devices facing Paseo del Yaque street as compared with average values among devices facing Majoma street (see black dots). The variables are CO, H2S, NH3, PM1, PM2.5, PM10, noise, and temperature. VOC Kilo Ohms or "kΩ" values were lower in devices facing Paseo del Yaque street, meaning comparatively higher concentrations detected.

For the analysis of Table 5 and Figure 12, devices were paired by order of alignment in their respective streets, departing from the northwest corner of the property. Considering values of

Table 4. Preliminary results for testing and initial approach. Total average of values between the 10th of January and the 11th of February, 2025.

Factor	Unit	Device 1	Device 2	Device 3	Device 4	Device 5	Device 6	Device 7	Device 8	*Th	Note	Ref.
CO	mg/m³	4.769	4.672	5.041	5.183	4.959	5.997	5.960	6.777	4	24-hour average	[22]
O3	µg/m³	19.94	19.95	19.89	20.19	20.04	19.87	20	20.04	60	Peak Season	[22]
H2S	ppb	2.57	2.55	2.56	2.58	2.61	2.50	2.70	2.6	14.35	Max. 90 days, = 20 µg/m³	[13]
NH3	µg/m³	3.04	2.96	2.98	2.98	2.97	3.32	2.99	3.01	270	24-hour mean	[16]
NO2	µg/m³	25.59	24.99	25.47	24.97	25.08	25.32	25.03	25.14	10	Annual average	[22]
VOCs	VOC index (sensor resistance proxy - kΩ)	424.26	233.1	43.41	69.28	26.71	31.92	32.25	23.20	?	Gas increases conductivity	[27]
PM1	µg/m³	2.065	2.232	2.098	2.095	2.829	3.735	3.30	3.44	2	= 0.002 mg/m³	[23]
PM2.5	µg/m³	4.126	4.49	4.01	3.85	4.92	6.62	6.01	5.69	5	Annual average	[22]
PM10	µg/m³	4.94	5.45	4.71	4.46	5.79	8.068	7.42	6.795	15	Annual average	[22]
Noise	dB	47.88	61.95	70.4	65.45	60.9	67.1	67.21	74.09	45/53	Night/day	[24]
TEMP	°C	27.23	26.07	25.81	26.57	28.5	26.9	26.92	25.87	26.6	"Caution Range": 80–90 °F.	[25]
RH	%RH	38.2	29.2	22	24	25.9	22.84	23.1	20	40-60	For occupied buildings	[26]

Note: "Th" stands for "threshold".

Table 5. Percent of increment by street

	CO	O3	H2S	NH3	NO2	VOCs	PM1	PM2.5	PM10	Noise	TEMP	RH
% Increment device Average devices 6,7,8 and 9, minus averages devices 3, 4, 1 and 2	20.48309	-0.02501	1.461988	2.759197	-0.44546	-85.1854	56.702	41.05365	43.52249	9.614132	2.375095	-19.0123
% Increment devices 6-3	18.96449	-0.10055	-2.34375	11.4094	-0.58893	-26.4686	78.02669	65.08728	71.29512	-4.6875	4.223169	3.818182
% Increment devices 7-4	14.99132	-0.94106	4.651163	0.33557	0.240288	-53.4498	57.5179	56.1039	66.36771	2.689076	1.317275	-3.75
% Increment devices 8-1	42.10526	0.501505	1.167315	-0.98684	-1.7585	-94.5317	66.58596	37.90596	37.55061	54.74102	-4.99449	-47.644
% Increment devices 5-2	6.142979	0.451128	2.352941	0.337838	0.360144	-88.5414	26.74731	9.576837	6.238532	-1.69492	9.321059	-11.3014

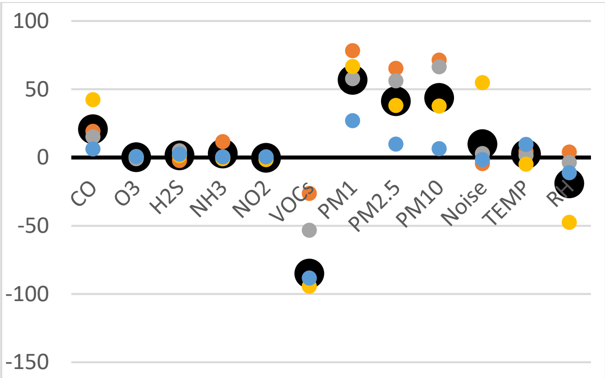

Figure 12. Percent of increment by street.

devices facing Majoma street as 100 % (devices 3, 4, 1, and 2), dots show percentage of increment between average values from devices: 6 and 3 (orange), 7 and 4 (grey), 8 and 1 (yellow), 5 and 2 (blue). Black dots represent increment in street average, that is, a comparison between averages of variables from devices that face the same street.

It is estimated that the segment of Paseo del Yaque street in front of the site has higher vehicle and pedestrian traffic. Additionally, that side of the property is from where most patients enter the healthcare facility.

Despite minor hardware attrition, the system architecture proved reliable, energy-efficient, and replicable for future stages. By transitioning from unmeasured assumptions to empirical data collection, this preliminary phase lays a robust foundation for broader, long-term monitoring and future information-based participatory planning in Los Ríos.

AUTHORS' CONTRIBUTION

The roles for each author, according to the CRediT taxonomy, available at https://credit.niso.org/, are described below:

Jesús D´Alessandro: conceptualization, formal analysis, investigation, methodology, supervision, visualization, writing – original draft, writing – review & editing.

Melisa Vargas: conceptualization, formal analysis, investigation, methodology, supervision, visualization, writing – review & editing.

Alfredo Sguglio: conceptualization, data curation, formal analysis, social investigation, methodology, software, supervision, validation, writing – review & editing.

Pierpaolo Fillippelli: conceptualization, data curation, formal analysis, investigation, methodology, software, supervision, validation, writing – review & editing.

Angelo Maciletti: conceptualization, data curation, formal analysis, investigation, methodology, software, supervision, validation, writing – review & editing.

David Feliz: data curation, software, supervision, validation.

ACKNOWLEDGEMENT

Ministerio de Educación Superior Ciencia y Tecnología de la República Dominicana funded the Project through Fondo Nacional de Innovación y Desarrollo Científico y Tecnológico (FONDOCYT), República Dominicana, Subvención No. 2022-3A2-154.

Fundación Altice provided SIM cards and telecommunication service to the devices, and covered travel expenses.

The Instituto Nacional de Diabetes, Endocrinología y Nutrición (INDEN) (Spanish for National Institute of Diabetes, Endocrinology and Nutrition) granted permission so the devices could be installed on its land, and provided electricity.

We thank Doctor Ammar Ibrahim, General Director of INDEN for his collaboration.

Illustrative urban footprint maps were drawn over maps from Google Maps.

We thank architect Victoria Escasena, who participated in research activities at the beginning of the project as an undergraduate student.

REFERENCES

[1] R. Holt, Global Cities: Which cities will be leading the global economy in 2035?, Oxford Economics (2018), pp. 1–15. Online [Accessed 27 August 2026] https://workplaceinsight.net/wp-content/uploads/2018/12/Global-Cities-Dec-2018.pdf

[2] OECD, Multi-dimensional Review of the Dominican Republic: Towards Greater Well-being for All, OECD Development Pathways, OECD Publishing, Paris, 2022 ISBN 978-92-64-55191-6 DOI: 10.1787/560c12bf-en

[3] P. Restrepo, D. Tello, Paving the Way for Prosperous Cities and Territories: Urbanization and Territorial Development Review of the Dominican Republic, World Bank, 2022, pp. 1–20. Online [Accessed 11 August 2026] https://documents1.worldbank.org/curated/en/099520007132233569/pdf/P172715065b95b0bc08ce70a7fe6442f014.pdf

[4] Ministerio de Economía, Planificación y Desarrollo (MEPYD), Mapa de la Pobreza de Republica Dominicana. Ministerio de Economía Planificación y Desarrollo (2014). Online [11 August 2026] [In Spanish] https://mepyd.gob.do/mepyd/wp-content/uploads/archivos/uaaes/mapa_pobreza/2014/Mapa%20de%20la%20pobreza%202014%2C%20informe%20general%2C%20editado%20final2%20FINAL.pdf

[5] Oficina Nacional de Estadística (ONE), Atlas de la situación sociodemográfica en la República Dominicana (Censo 2010), Santo Domingo, 2017. Online [Accessed 11 August 2026] [In Spanish]
https://one.gob.do/media/ekbjsskf/atlassituaci%C3%B3nsociodemogr%C3%A1ficaenlarepdomcenso2010feb2017.pdf

[6] Ayuntamiento del Distrito Nacional, Ordenamiento Territorial para el Desarrollo de Santo Domingo, Santo Domingo, 2019. Online [Accessed 20 August 2026] [In Spanish]
https://www.sismap.gob.do/Municipal/uploads/evidencias/637932272611839069-2.03_19-21_Plan-de-Ordenamiento-Territorial-DN..pdf

[7] Dirección General de Impuestos Internos, Parque Vehicular 2025, 2025. Online [Accessed 20 August 2026] [In Spanish]
https://dgii.gov.do/estadisticas/parqueVehicular/1Informes%20Parque%20Vehicular/ParqueVehicular2025.pdf

[8] Ayuntamiento del Distrito Nacional, Asentamientos Informales en el Distrito Nacional, 2023 [Accessed 11 August 2026] [In Spanish]
https://adn.gob.do/wpfd_file/asentamientos-informales-dn-informe-tecnico/

[9] CAASD. Plan Maestro del Alcantarillado Sanitario del Gran Santo Domingo
https://transparencia.caasd.gob.do/wp-content/uploads/2022/04/Plan-Maestro-Caasd-1.pdf

[10] F. Grullón, E. Rodriguez, M. Cairo, S. González, J. Rodríguez, R. Matos, E. López, R. Mesa, (+ 3 more authors), Assessment of short-lived climate pollutant mitigation in Dominican Republic: Recommendations for NDC Enhancement, National Council of Climate Change of the Dominican Republic (2021). Online [Accessed 20 August 2026]
https://www.ccacoalition.org/sites/default/files/resources//2021_SLCPs%20Report%20DR%20ENG.pdf

[11] V. Vaičiulis, J. Venclovienė, A. Miškinytė, R. Ustinavičienė, A. Dėdelė, G. Kalinienė, D. Lukšienė, A. Tamošiūnas, (+ 2 more authors), Association between outdoor air pollution and fatal acute myocardial infarction in Lithuania between 2006 and 2015: a time series design, International Journal of Environmental Research and Public Health 20 (2023) 5, p. 4549.
DOI: 10.3390/ijerph20054549

[12] B. Gu, L. Zhang, R. Van Dingenen, M. Vieno, H. J. Van Grinsven, X. Zhang, S. Zhang, Y. Chen, (+ 8 more authors), Abating ammonia is more cost-effective than nitrogen oxides for mitigating PM2.5 air pollution, Science 374 (2021) 6568, pp. 758–762.
DOI: 10.1126/science.abf8623

[13] C. Catlett, P. Beckman, N. Ferrier, H. Nusbaum, M. E. Papka, M. Berman, R. Sankaran, Measuring Cities with software-defined sensors, J. Soc. Comput. 1 (2020), pp. 14–27.
DOI: 10.23919/JSC.2020.0003

[14] A. G. Catalano, A. Sguglio, Cosenza: Trasformazioni urbane ed esplorazioni sociali. RubbettinoA. G. Catalano, A. Sguglio, Cosenza: Trasformazioni urbane ed esplorazioni sociali. Rubbettino, 2022, ISBN 884987359X, 9788849873597, pp. 129–147. [In Italian]

[15] A. Sguglio, N. Arcuri, R. Bruno, Integration of Social Science in Engineering Research for Smart Cities. The Italian Case of the RES NOVAE Project, Proc. of the 2018 IEEE International Conference on Environment and Electrical Engineering and 2018 IEEE Industrial and Commercial Power Systems Europe (EEEIC / I&CPS Europe), Palermo, Italy, 2018, pp. 1–6.
DOI: 10.1109/EEEIC.2018.8493774

[16] P. Beckman, R. Sankaran, C. Catlett, N. Ferrier, R. Jacob, M. E. Papka, Waggle: an open sensor platform for edge computing, Proc. of the 2016 IEEE Sensors, Orlando, USA, 2016, pp. 1–3.
DOI: 10.1109/ICSENS.2016.7808975

[17] Array of Things, University of Chicago. Online [Accessed 11 August 2026]
https://arrayofthings.github.io/

[18] R. Mitchum, Chicago becomes first city to launch Array of Things, University of Chicago, Chicago News (2016). Online [Accessed 11 August 2026]
https://news.uchicago.edu/story/chicago-becomes-first-city-launch-array-things

[19] ARGONNE National Laboratory, Array of Things: First at-scale research infrastructure deployment enabling researchers to study an urban environment, ARGONNE. Online [Accessed 11 August 2026]
https://www.anl.gov/mcs/array-of-things

[20] C. E. Catlett, P. H. Beckman, N. Ferrier, M. E. Papka, R. Sankaran, J. Solin, V. Taylor, D. Pancoast, (+ 1 more author), Hands-on computer science: The Array of Things experimental urban instrument, Comput. Sci. Eng. 24 (2022), pp. 57–63.
DOI: 10.1109/MCSE.2021.3139405

[21] C. E. Catlett, P. H. Beckman, R. Sankaran, K. K. Galvin, Array of things: a scientific research instrument in the public way: platform design and early lessons learned, Proc. of the 2nd International Workshop on Science of Smart City Operations and Platforms Engineering (SCOPE '17), Association for Computing Machinery, New York, USA, 2017, pp. 26–33.
DOI: 10.1145/3063386.3063771

[22] M. I. G. Daepp, A. Cabral, V. Ranganathan, V. Iyer, S. Counts, P. Johns, A. Roseway, C. Catlett, (+ 8 more authors), Eclipse: an end-to-end platform for low-cost, Hyperlocal environmental sensing in cities, Proc. of the 2022 21st ACM/IEEE International Conference on Information Processing in Sensor Networks (IPSN), Milano, Italy, 2022, pp. 28–40.
DOI: 10.1109/IPSN54338.2022.00010

[23] SAGE, About Sage: A new kind of NSF Mid-scale Research Infrastructure (MSRI) that supports AI at the Edge. Online [Accessed 11 August 2026]
https://sagecontinuum.org/about

[24] US National Science Foundation, Award Abstract # 1935984, Mid-Scale RI-1: SAGE: A Software-Defined Sensor Network. Online [Accessed 11 August 2026]
https://www.nsf.gov/awardsearch/showAward?AWD_ID=1935984

[25] D. Dematties, S. Rajani, R. Sankaran, S. Shahkarami, B. Raut, S. Collis, P. Beckman, N. Ferrier, Acoustic fingerprints in nature: a self-supervised learning approach for ecosystem activity monitoring, Ecological Informatics 83 (2024), p. 102823.
DOI: 10.1016/j.ecoinf.2024.102823

[26] R. C. Jackson, B. A. Raut, D. Dematties, S. M. Collis, N. Ferrier, P. Beckman, R. Sankaran, Y. Kim, (+ 3 other authors), ARMing the Edge: designing Edge computing–capable machine learning algorithms to target ARM doppler Lidar processing, Artificial Intelligence for the Earth Systems 2 (2023) 4, p. 220062.
DOI: 10.1175/AIES-D-22-0062.1

[27] B. A. Raut, P. Muradyan, R. Sankaran, R. C. Jackson, S. Park, S. A. Shahkarami, D. Dematties, Y. Kim, (+ 7 more authors), Optimizing cloud motion estimation on the Edge with phase correlation and optical flow, Atmospheric Measurement Techniques 16 (2023) 5, pp. 1195–1209.
DOI: 10.5194/amt-16-1195-2023

[28] D. Dematties, B. A. Raut, S. Park, R. C. Jackson, S. Shahkarami, Y. Kim, R. Sankaran, P. Beckman, (+ 2 more authors), Let's unleash the network judgment: a self-supervised approach for cloud image analysis, Artificial Intelligence for the Earth Systems (2023), pp. 1–34.
DOI: 10.1175/AIES-D-22-0063.1

[29] R. J. Cooper, N. Abgrall, G. Aversano, M. S. Bandstra, D. Hellfeld, T. H. Joshi, V. Negut, B. J. Quiter, (+ 13 more authors), Networked sensing for radiation detection, localization, and tracking, Journal of Physics: Conference Series 2586 (2023) 1, p. 12125.
DOI: 10.1088/1742-6596/2586/1/012125

[30] Y. Kim, S. Park, S. Shahkarami, R. Sankaran, N. Ferrier, P. Beckman, Goal-driven scheduling model in Edge computing for

smart city applications, Journal of Parallel and Distributed Computing 167 (2022), pp. 97–108.
DOI: 10.1016/j.jpdc.2022.04.024

[31] S. Park, Y. Kim, N. J. Ferrier, S. M. Collis, R. Sankaran, P. Beckman, Prediction of solar irradiance and photovoltaic solar energy product based on cloud coverage estimation using machine learning methods, Atmosphere 12 (2021) 3, p. 395.
DOI: 10.3390/atmos12030395

[32] P. Beckman, J. Dongarra, N. Ferrier, G. Fox, T. Moore, D. Reed, M. Beck, Harnessing the computing continuum for programming our world, in: Fog Computing: Theory and Practice. A. Zomaya, A. Abbas, S. Khan (editors). John Wiley & Sons, 2020, pp. 215–230.
DOI: 10.1002/9781119551713.ch7

[33] Environmental Research Group at Imperial College London, About the Breathe London network, Breathe London. Online [Accessed 20 August 2026]
https://www.breathelondon.org/about

[34] Mayor of London, Bloomberg Philanthropies, Imperial College London, Clarity, Breathe London: Case Studies and Best Practice Examples, C40 (2019). Online [Accessed 20 August 2026]
https://www.c40knowledgehub.org/s/article/Breathe-London?language=en_US

[35] A. Gómez, L. Guillermo Manzanillo, J. Vázquez, C. Quintana, Contaminación atmosférica en puntos seleccionados de la ciudad de Santo Domingo, República Dominicana, Ciencia y Sociedad 39 (2014) 3, pp. 533-557. Online [20 August 2026] [In Spanish].
https://www.redalyc.org/articulo.oa?id=87031897006

[36] M. J. Mendoza, A. A. Paniagua, C. Franco, U. Jauregui, A. Molina, Monitoreo y caracterización de los contaminantes atmosféricos a través de una red inalámbrica de sensores en las ciudades de Santo Domingo y Santiago de los Caballeros en la República Dominicana, Proc. of the XVII Congreso Internacional de Investigación Científica- Semana Dominicana de Ciencia y Tecnología, Santo Domingo, DR, 2022. Online [Accessed 11 August 2026] [In Spanish]
https://www.even3.com.br/anais/xviicic2022/485656-monitoreo-y-caracterizacion-de-los-contaminantes-atmosfericos-a-traves-de-una-red-inalambrica-de-sensores-en-las-/

[37] NASA, Data Services, NASA LARC POWER. Online [Accessed 20 August 2026].
https://power.larc.nasa.gov/docs/services/#:~:text=The%20POWER%20data%20products%20are,the%20same%20information%20multiple%20times

[38] C. William, C. H. Whitlock, P. W. Stackhouse, Determining wind resources as a function of surface roughness and height from NASA Global Assimilation Analysis, Proc. of the International Solar Energy Society 2005 Solar World Congress, 6-12 August 2005, Orlando, US.

[39] Zhengzhou Winsen Electronics Technology Co., "MQ136 Semiconductor Sensor for Hydrogen Sulfide," Datasheet. Online [Accessed 11 August 2026].
https://www.winsen-sensor.com/d/files/mq136-(ver1_6)---manual.pdf

[40] Zhengzhou Winsen Electronics Technology Co., "MQ131 Semiconductor Sensor for Ozone," Datasheet. Online [Accessed 20 August 2026].
https://cdn.sparkfun.com/assets/9/9/6/e/4/mq131-datasheet-low.pdf

[41] DFRobot, "Analog Sound Level Meter SKU: SEN0232," Datasheet. Online [Accessed 20 August 2026].
https://www.farnell.com/datasheets/3161978.pdf

[42] Analog Devices, "ADXL335: Small, Low Power, 3-Axis ±3 g Accelerometer," Datasheet. Online [Accessed 20 August 2026].
https://www.analog.com/media/en/technical-documentation/data-sheets/adxl335.pdf

[43] SGX Sensortech, "MiCS-6814 Compact MOS sensor for measuring pollution from automobile exhausts," Datasheet. Online [Accessed 11 August 2026].
https://www.sgxsensortech.com/content/uploads/2015/02/1143_Datasheet-MiCS-6814-rev-8.pdf

[44] Bosch Sensortec, BME680 Low power gas, pressure, temperature & humidity sensor, Datasheet. Online [Accessed 11 August 2026].
https://www.bosch-sensortec.com/media/boschsensortec/downloads/datasheets/bst-bme680-ds001.pdf

[45] Plantower, Digital universal particle concentration sensor PMS3003, Datasheet. Online [Accessed 20 August 2026].
https://www.dynamoelectronics.com/descargas/PMS3003.pdf?srsltid=AfmBOooEwYDWk-gYprD5E0_qQhV8DaHbprxgBm10bLy-LSa-XYFq0pdA

[46] C. H. Selene, J. Chou, Hydrogen Sulfide: Human Health Aspects, WHO, 2003, ISBN 92 4 153053 7. Online [Accessed 27 August 2026]
https://iris.who.int/handle/10665/42638

[47] C. Szabo, A timeline of hydrogen sulfide (H_2S) research: from environmental toxin to biological mediator, Biochemical Pharmacology 149 (2018), pp. 5-19.
DOI: 10.1016/j.bcp.2017.09.010

[48] B. Rani, U. Singh, A. K. Chuhan, D. Sharma, R. Maheshwari, Photochemical smog pollution and its mitigation measures, Journal of Advanced Scientific Research 2 (2011) 4, pp. 28-33. Online [Accessed 11 August 2026]
https://typeset.io/pdf/photochemical-smog-pollution-and-its-mitigation-measures-4l4omumee2.pdf

[49] WHO, 2000, ISBN 92-890-1358-3, Air Quality Guidelines for Europe, WHO Regional Publications, European Series, No. 91. Regional Office for Europe, Copenhagen. Online [Accessed 27 August 2026]
https://iris.who.int/bitstream/handle/10665/107335/9789289013581-eng.pdf?sequence=1&isAllowed=y

[50] S. Wang, J. Nan, C. Shi, Q. Fu, S. Gao, D. Wang, H. Cui, A. Saiz-Lopez, (+ 1 more author), Atmospheric ammonia and its impacts on regional air quality over the megacity of Shanghai, China, Sci Rep 5 (2015), p. 15842.
DOI: 10.1038/srep15842

[51] D. Saadi, E. Tirosh, I. Schnell, The relationship between city size and carbon monoxide (CO) concentration and their effect on heart rate variability (HRV), Int. J. Environ. Res. Public Health 18 (2021) 2, p. 788.
DOI: 10.3390/ijerph18020788

[52] D. Pal, S. K. Mitra, The environmental Kuznets curve for carbon dioxide in India and China: Growth and pollution at crossroad, Journal of Policy Modeling, 39 (2017) 2, pp. 371–385.
DOI: 10.1016/j.jpolmod.2017.03.005

[53] B. Barletta, S. Meinardi, F. Sherwood Rowland, C. Chan, X. Wang, S. Zou, Lo Yin Chan, D. R. Blake, Volatile organic compounds in 43 Chinese cities, Atmospheric Environment 39 (2005) 32, pp. 5979–5990.
DOI: 10.1016/j.atmosenv.2005.06.029

[54] R. D. Brook, S. Rajagopalan, Particulate matter, air pollution, and blood pressure, Journal of the American Society of Hypertension 3 (2009) 5, pp. 332–350.
DOI: 10.1016/j.jash.2009.08.005

[55] WHO, WHO global air quality guidelines, Particulate matter (PM2.5 and PM10), ozone, nitrogen dioxide, sulfur dioxide and carbon monoxide, WHO, 2021, ISBN 978-92-4-003422-8, pp. 31-32. Online [Accessed 11 August 2026]
https://iris.who.int/bitstream/handle/10665/345329/9789240034228-eng.pdf?sequence=1

[56] N. V. Zaitseva, S. V. Kleyn, K. V. Chetverkina, A. M. Andrishunas, M. Y. Tsinker, On the safe levels of micro-sized particles PM1.0 in ambient air // Hygiene and Sanitation, 103 (2024) 11, pp. 1434–1440.
DOI: 10.47470/0016-9900-2024-103-11-1434-1440

[57] WHO, Environmental Noise Guidelines for the European Region, WHO, 2018, ISBN 978-92-890-5356-3. Online [Accessed 20 August 2026].
https://www.who.int/publications/i/item/9789289053563

[58] D. Parker, National Emphasis Program – Outdoor and Indoor Heat-Related Hazards, OSHA-US Department of Labor. Online [Accessed 20 August 2026]. https://www.osha.gov/sites/default/files/enforcement/directives/CPL_03-00-024.pdf

[59] E. M. Sterling, A. Arundel, T. D. Sterling, Criteria for human exposure to humidity in occupied buildings. ASHRAE Trans. 91 (1985), pp. 611–622.

[60] A. M. Collier-Oxandale, J. Thorson, H. Halliday, J. Milford, M. Hannigan, Understanding the ability of low-cost MOx sensors to quantify ambient VOCs, Atmospheric Measurement Techniques 12 (2019) 3, pp. 1441–1460. DOI: 10.5194/amt-12-1441-2019